# Resonance Raman Spectroscopy of the Azurin His117Gly Mutant. Interconversion of Type 1 and Type 2 Copper Sites through Exogenous Ligands†

Tanneke den Blaauwen,‡ Carla W. G. Hoitink,‡ Gerard W. Canters,*,‡ Jane Han,§ Thomas M. Loehr,§ and Joann Sanders-Loehr*,§

*Gorlaeus Laboratories, Leiden University, 2300 RA Leiden, The Netherlands, and Department of Chemistry, Biochemistry, and Molecular Biology, Oregon Graduate Institute of Science & Technology, Portland, Oregon 97291-1000*

*Received June 11, 1993; Revised Manuscript Received September 14, 1993*⊛

ABSTRACT: The copper center of the *Pseudomonas aeruginosa* His117Gly azurin mutant is accessible to exogenous ligands through an aperture in its surface created by the removal of the endogenous imidazole ligand. Depending on the exogenous ligand, a surprising variety of type 1 and type 2 copper sites can be obtained that are readily distinguished by electronic, EPR, and resonance Raman (RR) spectroscopy. The RR spectrum of type 1 H117G with exogenous imidazole is nearly identical to that of wild-type azurin, indicating that the trigonal geometry and short Cu–S(Cys) bond of ~2.15 Å have been maintained. With anionic ligands (e.g., $Cl^-$, $Br^-$, $N_3^-$), the RR spectra show increased intensity at 370 and 400 $cm^{-1}$ and a corresponding decrease in intensity at 410 $cm^{-1}$, suggesting a lengthening of the Cu–S(Cys) bond as the site achieves a more tetrahedral character. An extreme example is the hydroxide adduct of H117G which is green in color and has optical and RR spectra reminiscent of the tetrahedral type 1 site in *Achromobacter cycloclastes* nitrite reductase. The fact that the basic RR pattern is little changed in most of the type 1 adducts indicates that the RR spectrum is due primarily to vibrations of the Cu-cysteinate moiety and that its coplanar conformation is conserved. Type 2 H117G proteins are formed by the addition of bidentate exogenous ligands such as histidine and histamine. They have their absorption maxima blue-shifted to 400 nm and their EPR $A_\parallel$ values increased to ~160 × $10^{-4}$ $cm^{-1}$, both of which are characteristic of tetragonal Cu sites with Cu–S(thiolate) bonds of >2.25 Å. The RR spectra of the type 2 H117G proteins are still dominated by multiple cysteinate-related vibrational modes. However, the vibrational modes with the greatest intensity and Cu–S(Cys) stretching character have shifted ~100 $cm^{-1}$ to lower energy compared to the type 1 sites, consistent with a longer (Cys)S–Cu bond. It is proposed that the tetragonal type 2 character of the bidentate ligand complexes is due to the addition of a fourth strong ligand in the equatorial ligand plane.

The cupredoxins are a class of mononuclear copper proteins that function in intermolecular electron transfer and that contain a blue (or type 1) copper site (Adman, 1985; Sykes, 1991). Type 1 Cu sites are characterized by an intense absorption band near 600 nm ($\epsilon$ = 3000–6000 $M^{-1}$ $cm^{-1}$ arising from (Cys)S → Cu(II) charge transfer and by EPR spectra with unusually small $A_\parallel$ values (<70 × $10^{-4}$ $cm^{-1}$) (Solomon et al., 1992). X-ray crystal structures for a number of cupredoxins have revealed that both the $\beta$-sandwich structure and the geometry of the copper site are highly conserved, irrespective of their biological origin (Adman, 1991). In all cases, the copper is coordinated to one cysteine and two histidines in a trigonal planar environment with a weaker axial ligand (generally methionine) at a longer distance. In the azurins, there is also a weakly interacting peptide carbonyl group (Baker, 1988; Nar et al., 1991a,b).

Another characteristic of type 1 Cu is that the ligating amino acids undergo very little structural rearrangement when the copper is removed or replaced by another metal ion (Garrett et al., 1984; Church et al., 1986; Shepard et al., 1990; Nar et al., 1992). This has led to the idea that the protein imposes a fairly rigid trigonal coordination geometry (Figure 1A) on the copper site (Williams, 1971; Gray & Malmström, 1983). The only obvious variability in these sites is the extent of displacement of the metal toward one of the weaker axial ligands (Figure 1B), generating a distorted tetrahedral

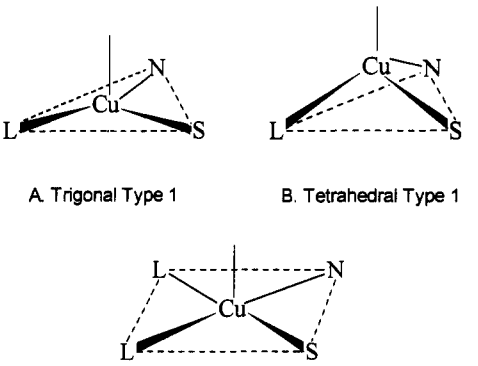


FIGURE 1: Proposed structures for type 1 and type 2 sites in H117G azurin. (A) The trigonal type 1 site has Cys112 (S), His46 (N), and an exogenous ligand (L) in a trigonal planar array. In wild-type, L = His117 with Met 121 as a weak axial ligand. (B) The tetrahedral type 1 site has Cu displaced from the trigonal ligand plane due to stronger coordination of the axial ligand. (C) The tetragonal type 2 site has four strong ligands [e.g., Cys 112 (S), His 46 (N), and a bidentate exogenous ligand (2L)] in a square planar array with one or more axial ligands at a longer distance. Based on Lu et al. (1993).

† This research was supported by the Technology Foundation (STW) of the Department of Economic Affairs, The Netherlands (T.d.B., G.W.C.), the Netherlands Foundation for Chemical Research (T.d.B., G.W.C.), and the U.S. Public Health Service, National Institutes of Health, Grant GM 18865 (T.M.L., J.S.-L.).

* To whom correspondence should be addressed.
‡ Leiden University.
§ Oregon Graduate Institute of Science and Technology.

⊛ Abstract published in *Advance ACS Abstracts,* November 1, 1993.

0006-2960/93/0432-12455$04.00/0 

geometry (Nar et al., 1992; Han et al., 1993; Lu et al., 1993). In contrast, removal of a cysteine or histidine ligand significantly increases the flexibility of the site, allowing the accommodation of up to four equatorial ligands (den Blaauwen et al., 1991; Mizoguchi et al., 1992). Such tetragonal sites (Figure 1C) fit the type 2 copper category because they lack strong absorption in the 600-nm region of the optical spectrum and have EPR $A_{\parallel}$ values $>100 \times 10^{-4}$ cm$^{-1}$. These properties are readily mimicked by ordinary tetragonal or square-planar copper complexes (Addison, 1985).

Azurin from *Pseudomonas aeruginosa* has proved to be particularly useful for these types of ligand replacement experiments. In the wild-type protein, the copper atom is surrounded by three strongly bonded donor groups in the equatorial plane: two $N_\delta$ from His46 and His117 and one $S_\gamma$ from Cys112 (Nar et al., 1991b). Two longer axial approaches (at ~3 Å) are made by the carbonyl oxygen from Gly45 and $S_\delta$ from Met121. This results in a distorted trigonal bipyramid in which the copper ion is displaced slightly (0.1 Å) out of the equatorial plane toward Met121. His117 protrudes through the surface of the protein (Nar et al., 1991b) and is thought to mediate electron transfer in the electron self-exchange reaction as well as in contacts with its physiological partners (van de Kamp et al., 1990a,b).

The His117 ligand of azurin can be replaced by glycine through site-directed mutagenesis (den Blaauwen et al., 1991). The absence of the amino acid side chain at position 117 creates an aperture in the surface of the protein which makes the copper center accessible to exogenous ligands without disturbing the protein structure (den Blaauwen & Canters, 1993). Addition of a monodentate ligand such as imidazole, halide ion, or azide regenerates the electronic and EPR spectral properties of a type 1 Cu site. Addition of a bidentate exogenous ligand such as histidine or histamine results in a species with a type 2 EPR spectrum and its major absorption band shifted to ~400 nm. These results suggest that the Cu binding site in cupredoxins is capable of accommodating a fourth ligand in the equatorial plane to generate a tetragonal coordination geometry. Similarly, replacement of the azurin Cys112 ligand with Asp also yields a tetragonal Cu site, presumably due to bidentate coordination by the new Asp112 ligand (Mizoguchi et al., 1992). This conversion from a type 1 to a type 2 site is presumably facilitated by the addition of a chelating ligand.

Resonance Raman (RR) spectroscopy is proving to be a useful method for investigating copper coordination geometry in azurin mutants. This technique specifically detects vibrational motions of bonded atoms when they are part of a chromophore (Nishimura et al., 1978) and, thus, is well suited to the analysis of copper thiolates. Cupredoxins exhibit a large number of RR bands between 250 and 500 cm$^{-1}$ that are believed to originate from kinematic and vibronic coupling of the Cu–S(Cys) stretch with vibrational motions of the cysteine and histidine ligands (Nestor et al., 1984; Blair et al., 1985). The unusually extensive coupling that occurs in these proteins appears to be related to the highly conserved coplanar arrangement of five atoms (Cu–$S_\gamma$–$C_\beta$–$C_\alpha$–N) in the copper–cysteinate moiety (Han et al., 1991). In the present study, we have found that all of the monodentate ligand adducts of H117G azurin have RR spectra typical of type 1 Cu sites, thereby confirming a conserved Cu(II) coordination geometry. In contrast, the bidentate ligand adducts of H117G yield novel RR spectra upon excitation within their 400-nm absorption bands. These spectra are indicative of a lengthening of the Cu–S(Cys) bond, as would be expected from the addition of a fourth ligand to the equatorial plane to form a type 2 Cu site. When the accompanying weaker 630-nm absorption band of the bidentate adducts is probed by RR spectroscopy, only a type 1 spectrum is observed. We postulate that the H117G mutant can coordinate an exogenous bidentate ligand in either a monodentate or bidentate fashion, thereby generating a mixture of type 1 and type 2 species.

## EXPERIMENTAL PROCEDURES

*Materials.* Imidazole (Imid), thiazole, $NaN_3$, NaCl, NaBr, and NaSCN were purchased from E. Merck AG, Darmstadt, Germany, histidine (His) was purchased from Sigma Chemical Co., St. Louis, MO, and histamine (Hista) was purchased from Janssen Chimica, Beerse, Belgium. The wild-type (WT) protein and the His117Gly (H117G) mutant of *Pseudomonas aeruginosa* azurin were expressed in *Escherichia coli* and purified as described previously (den Blaauwen et al., 1991). The WT and Met121Gln forms of *Alcaligenes denitrificans* azurin were prepared from protein expressed in *E. coli* (Hoitink et al., 1992).

*Preparation of H117G Azurin with Exogenous Ligands.* A stoichiometric amount of $Cu(NO_3)_2$ was added to a 0.1 mM apo-H117G solution in 20 mM MES buffer (pH 6.0). After 30 min of incubation, a 30-fold excess of ligand was added to the solution. The spectrum obtained after the absorption had maximized was used to calculate the extinction coefficient of the copper chromophore, with the protein concentration being based on $\epsilon_{280}$ = 9800 M$^{-1}$ cm$^{-1}$ (den Blaauwen et al., 1991). For RR spectroscopy, samples were concentrated to 2 mM in an ultrafiltration cell with a PLGC 10000 NMWL membrane (Millipore Corporation). In cases where no exogenous ligand was added to H117G azurin, the copper is assumed to be coordinated to one or more solvent molecules and is referred to as H117G($H_2O$), prepared at pH 6.0, or H117G(OH), prepared in 20 mM CHES buffer (pH 9.0).

*Spectroscopy.* UV/vis spectra were recorded on a Cary 219 spectrophotometer (Varian). EPR spectra were obtained as described previously (den Blaauwen & Canters, 1993). Resonance Raman (RR) spectra were obtained with a computer-interfaced Jarrell-Ash spectrophotometer using either a Spectra Physics 2025-11 (Kr), Spectra Physics 164 (Ar), or Coherent Innova 90-6 (Ar)/599-01 (rhodamine 6G) dye laser. The detector was an RCA C31034 photomultiplier tube with an ORTEC model 9302 amplifier/discriminator. The Raman spectra were collected in an ~150° backscattering geometry with samples maintained at ~15 K in a closed-cycle helium refrigerator (Air Products Displex). For comparison of mutant and WT azurins, samples were run consecutively under identical instrumental conditions. Frequencies are accurate to ±1 cm$^{-1}$.

## RESULTS AND DISCUSSION

A recent analysis of a series of cupredoxins has led to the conclusion that electronic and EPR spectral properties can be used to distinguish copper-site geometry (Han et al., 1993; Romero et al., 1993; Lu et al., 1993). Thus, type 1 sites with the Cu in close proximity to the $(His)_2Cys$ trigonal ligand plane (Figure 1A) are characterized by an axial EPR spectrum and a weak absorption band at 460 nm, the ratio of $\epsilon_{460}$ to $\epsilon_{600}$ ($R_{abs}$) being less than 0.1. Conversely, type 1 sites with a tetrahedral distortion in which the Cu has moved away from the $(His)_2Cys$ plane and toward one of the axial ligands (Figure 1B) are characterized by a rhombic EPR spectrum and an increased absorbance at 460 nm, with $R_{abs}$ values ranging from 0.2 to 1.3. Resonance Raman spectra are less sensitive

Table I: Electronic and EPR Spectra of His117Gly Azurin with Exogenous Ligands

| | absorption bands[b] | | | EPR signal[c] |
|---|---|---|---|---|
| ligand[a] | λ (ε) | λ (ε) | λ (ε) | $A_\parallel$ ($10^{-4}$ cm$^{-1}$) |
| type 1 Cu site | | | | |
| wild-type | | 465 (0.2) | 628 (5.7) | 58 |
| imidazole | | 460 (0.2) | 626 (4.5) | 85 |
| thiazole | | *d* | 632 (3.8) | 85 |
| histidine-1 | | | 634 (7%)[e] | |
| histamine-1 | | | 634 (17%)[e] | 78 |
| $Cl^-$ | | 470 (0.4) | 648 (4.9) | 17 |
| $SCN^-$ | 415 (0.1) | 455 (0.2) | 660 (4.7) | 17 |
| $N_3^-$ | 435 (0.9) | 490 (1.0) | 670 (4.7) | 21 |
| $Br^-$ | 338 (2.0) | 485 (0.9) | 683 (5.5) | 52 |
| aqua-1 | | | 628 (24%)[e] | |
| hydroxo-1B | | | 620 (nd) | |
| hydroxo-1G | | 440 (nd) | 540 (nd) | |
| type 2 Cu site | | | | |
| histidine-2 | 400 (36%)[e] | | | 156 |
| histamine-2 | 402 (69%)[e] | | | 162 |
| aqua-2 | 420 (33%)[e] | | | 139 |
| hydroxo-2 | 400 (nd) | | | |

[a] Species 1 and 2 are components of an equilibrium mixture. [b] $\lambda_{max}$ in nm, ε in mM$^{-1}$ cm$^{-1}$ at the indicated wavelength is a lower limit based on the $\epsilon_{280}$ = 9.8 mM$^{-1}$ cm$^{-1}$ value for wild-type. nd = not determined. All samples were in 20 mM MES (pH 6.0) except for His117Gly(OH) which was in 20 mM CHES (pH 9.0). [c] Measured at 77 K on samples in 16 mM MES and 40% glycerol (pH 6.2). [d] This peak is obscured by the aqua-2 species due to the weak binding of thiazole. [e] Since the relative abundances of species 1 and 2 are not known, their absorption intensities are expressed as percentage of the 628-nm absorption for WT (at an equivalent $A_{280}$ protein concentration).

to variability in axial-ligand bond strength, presumably because this bond is too long to have a measurable vibrational frequency (Thamann et al., 1982). Rather, RR spectra are primarily indicators of the properties of the Cu–cysteinate moiety, i.e., the strength of the Cu–S(Cys) bond and the coplanarity of the cysteinate backbone (Han et al., 1991). The Cu–$S_\gamma$–$C_\beta$–$C_\alpha$–N plane lies perpendicular to the Cu-equatorial ligands (Han et al., 1991) and is apparently not disturbed by copper displacements along the axial-ligand axis.

*Type 1 with Exogenous Imidazole.* Reconstitution of the His117Gly azurin mutant with copper and imidazole, H117G-(Imid), yields a type 1 Cu site that is remarkably similar to that of WT azurin (den Blaauwen & Canters, 1993). The electronic spectrum of H117G(Imid) exhibits absorption maxima at 460 and 626 nm and an $R_{abs}$ of 0.04, all of which are close to the WT values of 465 and 628 nm and an $R_{abs}$ of 0.04 (Table I, Figure 2A). The EPR spectrum of H117G-(Imid) is clearly axial (Figure 3A) as is that of WT, but its $A_\parallel$ of 85 × $10^{-4}$ cm$^{-1}$ is somewhat larger than the value of 58 × $10^{-4}$ cm$^{-1}$ for WT (Table I). The axial EPR spectrum and the low value for $R_{abs}$ indicate that the trigonal planar orientation of the three strong ligands, N(His 46), S(Cys 112), and N(Imid), has been maintained. Thus, the imidazole ring of the exogenous ligand in H117G(Imid) must be occupying a position similar to that of the imidazole ring of His117 in the WT protein.

A particularly notable aspect of the H117G–azurin complex with exogenous imidazole is that its RR spectrum is almost identical to that of WT (Figure 4A, B). This indicates that the Cu–cysteinate orientation of WT is highly conserved in H117G(Imid). Apparent differences are a –2-cm$^{-1}$ shift in the peak at 284 cm$^{-1}$ and increased intensity in the shoulder at 399 cm$^{-1}$. The 284-cm$^{-1}$ mode has been assigned as a Cu–N(imidazole) stretch on the basis of its copper- and deuterium-isotope dependence (Nestor et al., 1984; Blair et al., 1985). The decreased frequency of this mode in H117G(Imid)

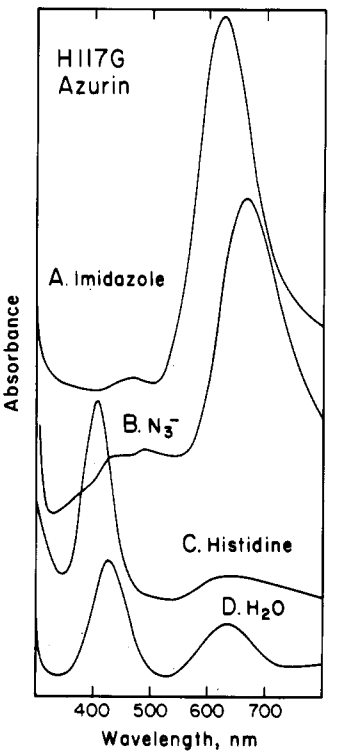


FIGURE 2: Electronic spectra of H117G azurin plus exogenous ligands. Apoprotein (~0.1 mM) was incubated with a stoichiometric amount of Cu in 20 mM MES (pH 6.0) plus (A) imidazole, (B) azide, and (C) histidine (all in a 30-fold excess) or (D) $H_2O$ (no ligand added).

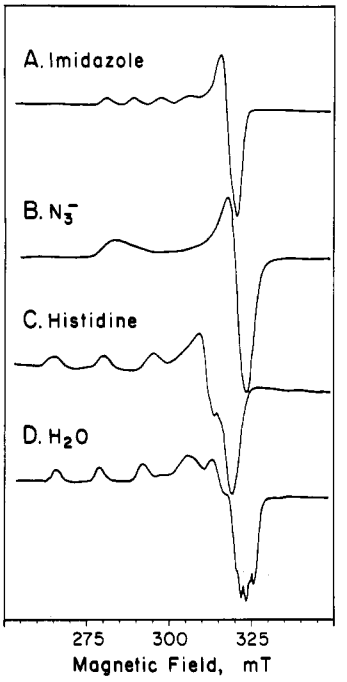


FIGURE 3: EPR spectra of H117G azurin plus exogenous ligands. Samples in 16 mM MES and 40% glycerol (pH 6.2) were prepared as in Figure 2 and then washed with 200 mM NaCl to remove adventitious Cu and concentrated to 2 mM protein. The spectra were recorded at 77 K with a JEOL JESS-RE2X spectrometer operating at X-band frequencies and interfaced to an ESPRIT330 data system. Parameters for recording the EPR spectra were 12.5 mT/min sweep rate, 0.63 mT modulation amplitude, 8.950 GHz frequency, and 5 mW incident microwave power. The magnetic field was calibrated with DPPH (α,α′-diphenyl-β-picrylhydrazyl).

suggests a slightly longer bond (Δ < 0.01 Å) to the exogenous imidazole (Herschbach & Laurie, 1961). The increase in intensity at 399 cm$^{-1}$ and concomitant decrease in intensity

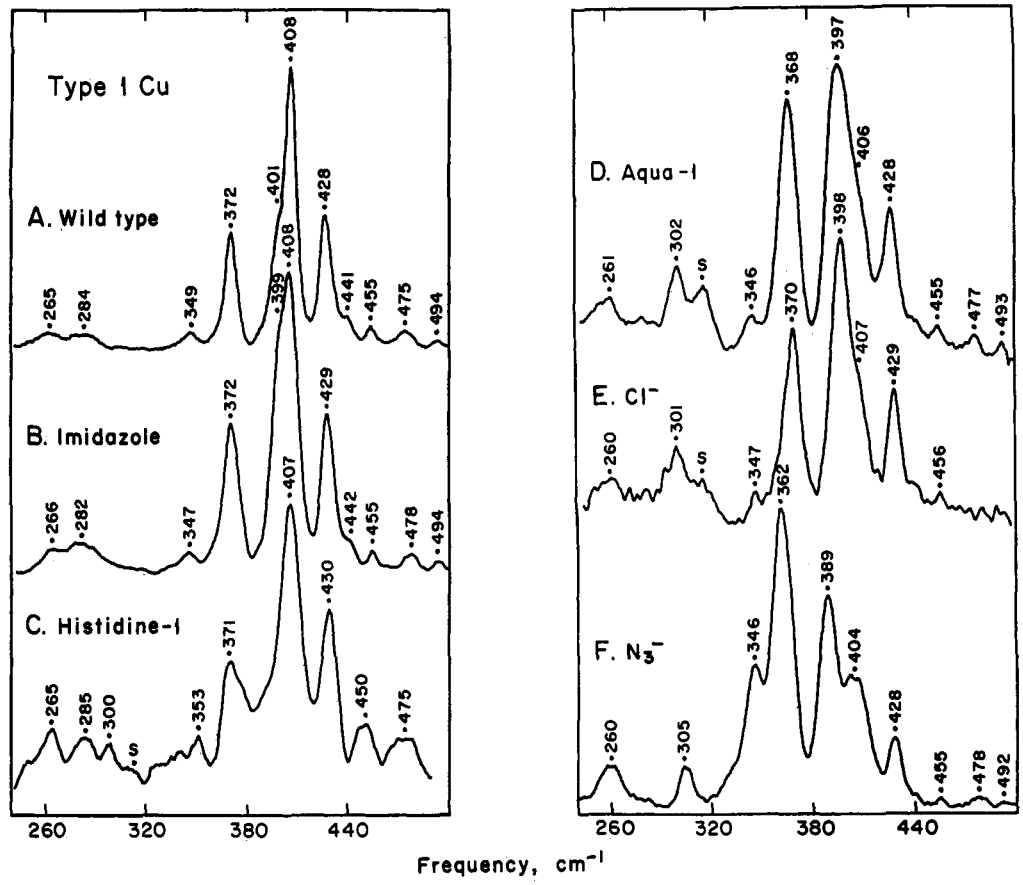


FIGURE 4: Resonance Raman spectra of type 1 sites in H117G azurins obtained with 647.1-nm excitation. (A) Wild-type, (B) H117G plus imidazole, (C) H117G plus histidine, (D) H117G at pH 6.0 (no ligand added), (E) H117G plus chloride, and (F) H117G plus azide. Spectra were obtained on samples (~2 mM) in 20 mM MES, pH 6.0, at 15 K using a power of 70–100 mW, resolution of 5 $cm^{-1}$, scan rate of 0.5 $cm^{-1}/s$, and accumulations of 4–9 scans.

at 408 $cm^{-1}$ is also indicative of a slight lengthening of the Cu–S(Cys) bond.

*Effect of Cu–S(Cys) Bond Length.* As suggested earlier (Blair et al., 1985), the peaks with the greatest Raman intensity appear to have the greatest Cu–S(Cys) stretching character and, thus, serve as indicators of Cu–S bond strength. This has recently been verified by growing *P. aeruginosa* azurin on [$^{34}$S]sulfate and determining the pattern of S-isotope dependence (Dave et al., 1993). In WT azurin, the most intense feature at 408 $cm^{-1}$ shows the largest shift to lower energy, with an additional small shift being detected for the peak at 428 $cm^{-1}$. Thus, the cysteinate-deformation modes at 408 and 428 $cm^{-1}$ are the modes that are most strongly coupled with the Cu–S stretch. A different pattern is observed for the *P. aeruginosa* azurin mutant in which the His46 ligand has been replaced by aspartate (Chang et al., 1991). In that case, the predominant sulfur-isotope dependence has shifted to the peak at 400 $cm^{-1}$, consistent with its having become the most intense feature in the RR spectrum (Dave et al., 1993). An additional indicator of Cu–S stretching character comes from an analysis of combination bands in the 700–900-$cm^{-1}$ region. In WT azurin, the majority of the combination bands are generated by the 408-$cm^{-1}$ fundamental (Blair et al., 1985) whereas, in the His46Asp azurin mutant, they are based on the 400-$cm^{-1}$ fundamental (Dave et al., 1993). Electronic and EPR spectra indicate that the His46Asp mutation has caused the type 1 Cu site to shift from a trigonal to a tetrahedral geometry (Germanas et al., 1993; Dave et al., 1993), most likely owing to stronger coordination of the axial methionine ligand (Lowery & Solomon, 1992). The RR results suggest that this conversion from a trigonal to a tetrahedral type 1 site is accompanied by a slight lengthening of the Cu–S(Cys) bond ($\Delta < 0.02$ Å) which causes the Cu–S(Cys) stretch to couple to a greater extent with lower energy deformation modes.

A similar shift in vibrational intensities is observed for the Met121Gln mutant of *Alcaligenes denitrificans* azurin. The RR spectrum of the WT protein (Figure 5A) differs somewhat from that of *P. aeruginosa* azurin (Figure 3A) in its intensity pattern, and the peaks in the 360–500-$cm^{-1}$ region are typically 1–5 $cm^{-1}$ higher in energy. Substitution of the axial Met 121 ligand with Gln results in increased RR intensity at 373 and 396 $cm^{-1}$ and decreased RR intensity at 413 and 429 $cm^{-1}$ (Figure 5B). This again implies enhanced coupling of the Cu–S stretch with lower energy cysteinate deformation modes. According to both the X-ray structure and the EPR spectrum, Met121Gln azurin contains a tetrahedral type 1 site due to the stronger binding of Cu to the carbonyl group of the glutamine ligand (Romero et al., 1993). The coupling to RR modes 10–40 $cm^{-1}$ lower in energy (as reflected by the redistribution of intensities) and the 1–2-$cm^{-1}$ lowering of most of the fundamentals suggests a 0.01–0.04-Å increase the Cu–S(Cys) bond length (Herschbach & Laurie, 1961). A similar increase in the Cu–N(His117) bond length is indicated by the 7-$cm^{-1}$ shift of the 283-$cm^{-1}$ mode to lower energy. It is unlikely that such changes in bond distances would be detected in an X-ray crystal structure since they fall within the ±0.05 Å error limit (Guss et al., 1992). In contrast, RR spectra appear to be sensitive indicators of these small changes in Cu–S and Cu–N coordination.

*Type 1 Cu with Exogenous Anions.* Reconstitution of H117G with a variety of anions such as $Cl^-$, $SCN^-$, $N_3^-$, and

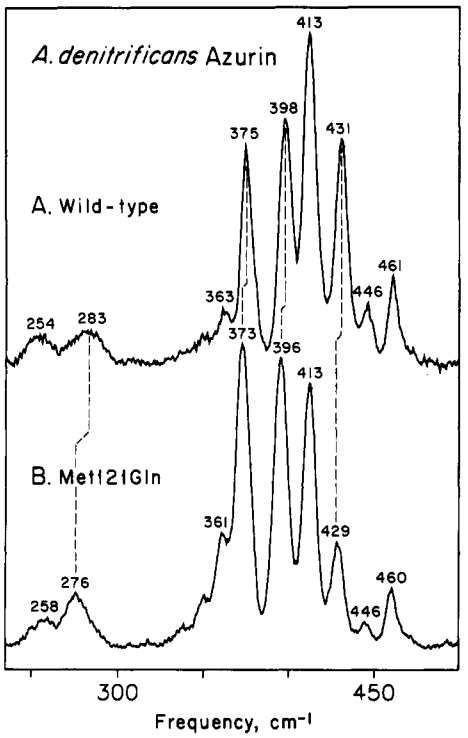


FIGURE 5: Resonance Raman spectra of azurins from *Alcaligenes denitrificans*. (A) Wild-type and (B) Met121Gln mutant. Spectra were obtained on ~2 mM samples in 10 mM Tris-HCl (pH 8.0) under conditions as given in the legend to Figure 4.

$Br^-$ again yields typical type 1 Cu characteristics. The electronic spectra still exhibit the type 1 pattern of an intense (Cys)S → Cu(II) CT band at ≥620 nm and a weak shoulder at ≥450 nm, but the absorption maxima of the main bands have undergone substantial red-shifts of 20–55 nm (Figure 2B, Table I). The shifts in going from $Cl^-$ to $SCN^-$ to $N_3^-$ to $Br^-$ are in the order expected from the spectrochemical series, yielding a lower energy of the copper terminal d orbital with weaker ligand-field strength (den Blaauwen & Canters, 1993). The EPR spectra for the $Cl^-$, $SCN^-$, and $N_3^-$ complexes exhibit extremely small $A_\parallel$ values of $\leq 20 \times 10^{-4}$ $cm^{-1}$ (Table I, Figure 3B). The $g_\parallel$ to $A_\parallel$ ratio for all four anionic complexes (den Blaauwen & Canters, 1993) places them clearly in the type 1 Cu category.

The RR spectrum of the $Cl^-$ adduct of H117G azurin (Figure 4E, Table II) is surprisingly similar to that of H117G(Imid). Most of the peaks have similar frequencies and intensities. The major changes relative to WT are (i) shifts of –2 to –4 $cm^{-1}$ for the peaks at 260, 370, and 398 $cm^{-1}$, (ii) increased intensity at 370 and 398 $cm^{-1}$, (iii) loss of the peak at 282 $cm^{-1}$, and (iv) appearance of a new mode at 301 $cm^{-1}$. *The fact that the RR spectrum is so little altered by the removal of an imidazole ligand suggests that it arises primarily from vibrations of the Cu–S(Cys) moiety.* Similarly, substitution of the other His ligand, His46, by aspartate causes very little change in the RR spectrum, except for increased intensity at 399 $cm^{-1}$ (Dave et al., 1993). The RR frequencies for the $Br^-$ and $SCN^-$ complexes (Table II) are close to those of the $Cl^-$ complex. In the $Br^-$ complex, the 399-$cm^{-1}$ peak is the most intense spectral feature, as with $Cl^-$ (Figure 4E), whereas in the $SCN^-$ complex the 397-$cm^{-1}$ feature is only a shoulder, as with imidazole (Figure 4B). The most extreme behavior is exhibited by the $N_3^-$ complex where the peaks at ~370 and ~400 $cm^{-1}$ are shifted to 362 and 389 $cm^{-1}$, respectively, with the 362-$cm^{-1}$ mode having become the most intense feature in the spectrum (Figure 4F).

The above data show that replacement of the imidazole at position 117 with anions tends to increase the intensity of the peak near 400 $cm^{-1}$, with a corresponding decrease in the intensity of the peak near 410 $cm^{-1}$. The similar intensity change for the His46Asp azurin mutant has been ascribed to an increase in Cu–S bond length which causes the dominant Cu–S stretch to couple with lower energy deformation modes (Dave et al., 1993). It is likely that the increased intensity near 400 $cm^{-1}$ for the $Cl^-$ and $Br^-$ complexes of H117G azurin is also due to a slight lengthening of the Cu–S(Cys) bond. This idea is supported by the fact that the 399-$cm^{-1}$ peak of the $Br^-$ complex is the major generator of combination bands at higher energy (C. R. Andrew, J. Sanders-Loehr, and G. W. Canters, unpublished results). For the $N_3^-$ complex of H117G, the RR spectrum shows larger frequency shifts of ~10 $cm^{-1}$ with the predominant $\nu$(Cu–S) mode probably shifted to 362

Table II: Resonance Raman Spectra of His117Gly Azurin with Exogenous Ligands[a]

| ligand | RR frequencies ($cm^{-1}$) | | | | | | | | | | | |
|---|---|---|---|---|---|---|---|---|---|---|---|---|
| type 1 Cu sites[b] | | | | | | | | | | | | |
| wild-type | 267 | 284 | | | 348 | 372 | 401 | **408** | 428 | 456 | 476 | 494 |
| imidazole | 266 | 282 | | | 347 | 372 | 399 | **408** | 429 | 455 | 478 | 494 |
| 4-MeImid | 259 | | | | 349 | 373 | 400 | **407** | 429 | 455 | 477 | 494 |
| *N*-polyvinylImid | 267 | 283 | | | 348 | 372 | 400 | **407** | 429 | 455 | 477 | 494 |
| thiazole | 260 | | 303 | | 347 | 371 | 400 | **410** | 430 | 456 | 478 | 494 |
| histidine-1 | 266 | 286 | 300 | | 352 | 372 | | **408** | 431 | 451 | 471 | |
| histamine-1 | 262 | 284 | 304 | | 347 | 370 | 398 | **406** | 429 | 456 | 478 | 493 |
| $Cl^-$ | 260 | | 301 | | 347 | 370 | **398** | 407 | 429 | 457 | 482 | 494 |
| $SCN^-$ | 262 | 283 | 292 | | 348 | 371 | 397 | **403** | 428 | 455 | 471 | 494 |
| $N_3^-$ | 259 | | 305 | | 346 | **362** | **389** | 402 | 428 | 455 | 478 | 493 |
| $Br^-$ | 261 | 285 | 305 | | | 370 | **399** | **408** | 430 | 457 | 480 | 494 |
| aqua-1 | 260 | | 302 | | 346 | **368** | **397** | 407 | 428 | 456 | 477 | 493 |
| hydroxo-1B | | | 304 | | 348 | **366** | 393 | 409 | 428 | 455 | 476 | 493 |
| hydroxo-1G | | | 286 | | | **365** | 399 | 412 | 426 | | | |
| type 2 Cu sites[c] | | | | | | | | | | | | |
| histidine-2 | 261 | | **298** | **319** | 351 | | 385 | 391 | 426 | | | |
| histamine-2 | 268 | | 298 | **319** | 348 | | 385 | | 434 | | | |
| aqua-2 | 267 | | **298** | **317** | 352 | 362 | 387 | 404 | 426 | | | |
| hydroxo-2 | 271 | | 295 | **312** | 350 | 368 | 376 | 400 | 430 | | | |

[a] Boldface numbers denote the most intense peak(s) in the spectrum. [b] RR spectra for all species were obtained with 647.1-nm excitation (as in Figure 4) except for the hydroxo-1G species which was obtained with 457.9-nm excitation (as in Figure 8). [c] RR spectra were obtained with 413.1-nm excitation (as in Figure 6).

$cm^{-1}$ (Figure 4F), indicating a greater lengthening of the Cu–S bond.

The $SCN^-$ complex has an additional absorption band at 415 nm (Table I) which is most likely a $SCN^- \rightarrow Cu(II)$ CT band. Similarly, the $N_3^-$ complex has an additional absorption band at 435 nm (Table I) assignable to $N_3^- \rightarrow Cu(II)$ CT. Excitation of the $N_3^-$ complex at 413.1 nm yields a new RR peak at 2055 $cm^{-1}$ (data not shown) that is characteristic of the asymmetric N–N–N stretch of a terminally coordinated azide (Pate et al., 1989). However, no new spectroscopic features assignable to the Cu–N stretch of a bound azide could be detected between 200 and 500 $cm^{-1}$ using 413.1-nm excitation.

*Cu–Imidazole Vibrations.* The peak at 284 $cm^{-1}$ in WT azurin and other type 1 Cu proteins has been assigned as a Cu–N(imidazole) stretch (with the entire imidazole ring behaving as a point mass of 68) on the basis of its ~2-$cm^{-1}$ shift to lower energy upon substitution of $^{65}Cu$ for $^{63}Cu$ or substitution of D for H (Nestor et al., 1984; Blair et al., 1985). We have verified the Cu isotope dependence of this mode using the azurin H117G(Imid) complex (Sanders-Loehr, 1993). Furthermore, the 284-$cm^{-1}$ mode disappears when the exogenous imidazole of H117G is replaced by other ligands such as $Cl^-$, $N_3^-$, and thiazole (Figure 4, Table II). The question remains as to how much the imidazole ligand at position 117 contributes to the multitude of other features in the RR spectrum. The $Cl^-$, $Br^-$, and $SCN^-$ complexes of H117G show very little additional spectral change accompanying the loss of this imidazole ligand, and the small frequency and intensity changes that are observed can be accounted for by concomitant changes in ligand field and coordination geometry. The thiazole adduct, which is chemically more similar to imidazole, gives an RR spectrum essentially identical to that of H117G(Imid) (Table II). Since imidazole ring vibrations are very different from those of thiazole, neither seems to be contributing significantly to the RR spectrum. This conclusion is supported by the finding that when H117G(Imid) is prepared with [$^{15}N$]imidazole, the only vibrational fundamental affected by the isotope substitution is the peak at 282 $cm^{-1}$ (Sanders-Loehr, 1993).

The imidazole ligand of His 46 appears to have even less effect on the RR spectrum. The azurin H46D mutant shows no loss of intensity of 284 $cm^{-1}$, and the other small spectral changes can be accounted for by the increased Cu–S(Cys) bond length associated with a more tetrahedral type 1 site (Dave et al., 1993). The reason for the apparently greater contribution of H117 than H46 to the RR spectrum is not clear. The crystal structure of WT azurin (H. Nar, personal communication) shows that both of the imidazole rings are twisted with respect to the Cu–NNS plane, giving dihedral angles of ~40° for H117 and ~20° for H46.

The H117G mutant can also bind a number of imidazole derivatives such as 2-methyl-, 4-methyl-, *N*-methyl-, and *N*-polyvinylimidazole. These derivatives have electronic and EPR spectra close to those of WT, indicating that a type 1 Cu site has again been generated (den Blaauwen & Canters, 1993). The RR spectra of the H117G complexes with these modified imidazoles are highly similar to the spectrum of H117G(Imid) (Table II). All have an essentially identical pattern of frequencies and intensities above 300 $cm^{-1}$. The 283-$cm^{-1}$ mode is observed for the H117G complexes with *N*-polyvinylimidazole (Table II) and 2-methylimidazole (data not shown) but not with 4-methylimidazole (Table II) or *N*-methylimidazole (data not shown). It is possible that subtle differences in imidazole orientation affect orbital overlap and, hence, vibronic coupling with the (Cys)S → Cu(II) CT transition. However, such interpretations regarding the 284-$cm^{-1}$ peak must be made with caution. Several H117G adducts, including $Br^-$ and $SCN^-$, still have intensity in the 284-$cm^{-1}$ region (Table II), indicating that there may also be a contribution from a Cu–cysteinate mode at this frequency.

*Type 1 and Type 2 with Bidentate Ligands.* Complexes of H117G azurin with exogenous histidine, H117G(His), or histamine, H117G(Hista), have unusual spectroscopic properties (den Blaauwen & Canters, 1993). Both complexes exhibit strong absorption at 400 nm and weaker absorption at 634 nm (Table I, Figure 2C). The extinction coefficient for the 400-nm band appears to be in the 2000–4000 $M^{-1}$ $cm^{-1}$ range and, thus, still characteristic of (Cys)S → Cu(II) CT; however, the high energy is more typical of type 2 Cu (Han et al., 1993). The EPR spectra of H117G(His) and H117G(Hista) verify that the major component in each sample is indeed a type 2 Cu species, referred to as histidine-2 and histamine-2, respectively (Figure 3C, Table I). The most likely explanation for these new species is that the exogenous ligands are bound in a *bidentate* fashion, with both the imidazole and the amine nitrogen atoms coordinated, thereby conferring a tetragonal type 2 geometry onto the copper site (Figure 1C). Even though the Cu site can accommodate a bidentate ligand, a fraction of the azurin molecules still bind the bidentate ligands in a *monodentate* fashion. These type 1 species, referred to as histidine-1 and histamine-1, give rise to the 634-nm absorption and possess a typical type 1 RR spectrum.

Excitation of H117G(His) within the 634-nm absorption band yields a RR spectrum (Figure 4C) that is close to the spectrum of WT azurin. This shows that the absorption at 634 nm is due to a type 1 Cu site and that the imidazole moiety of histidine is the most probable ligand donor. The only distinctive spectral difference between the histidine-1 component and WT azurin is the appearance of an additional RR peak at 300 $cm^{-1}$ (Figure 4C). Peaks at this frequency are routinely observed in many other H117G adducts (e.g., anions, thiazole), and, thus, a 300-$cm^{-1}$ feature is yet another vibrational indicator of a type 1 Cu site (Table II). On the basis of the absorbance at 634 nm, the histidine-1 species represents <10% of the total bound histidine (Table I), and it is not detected in the EPR spectrum (Figure 3C). The strong resonance enhancement of type 1 Cu sites makes it possible to detect this minor component with 647.1-nm excitation. The H117G complex with histamine also shows a RR spectrum typical of type 1 Cu with red excitation (Table II). Its absorption spectrum indicates that the histamine-1 species makes up >10% of the total bound histamine (Table I), and, in this case, the EPR spectrum does indicate the presence of a minor type 1 component (Table I).

For H117(His) and H117G(Hista), maximum absorbance at 634 nm is achieved at pH 5, whereas maximum absorbance at 400 nm requires a pH >7. Thus, it is the deprotonation of the amine that leads to bidentate coordination. Excitation within the 400-nm absorption bands of these two complexes leads to significantly altered RR spectra with the most intense peaks between 295 and 320 $cm^{-1}$ (Figure 6A,B; Table II). These spectra are assigned to the type 2 component in each sample. The RR spectra still show a large number of vibrational modes, and these occur at approximately the same frequencies as in the type 1 RR spectra. Similarly, in the high-frequency region, the histidine-2 component reveals a C–S stretch at 763 $cm^{-1}$ and additional cysteinate fundamentals at 1234 and 1424 $cm^{-1}$ (C. R. Andrew, J. Sanders-

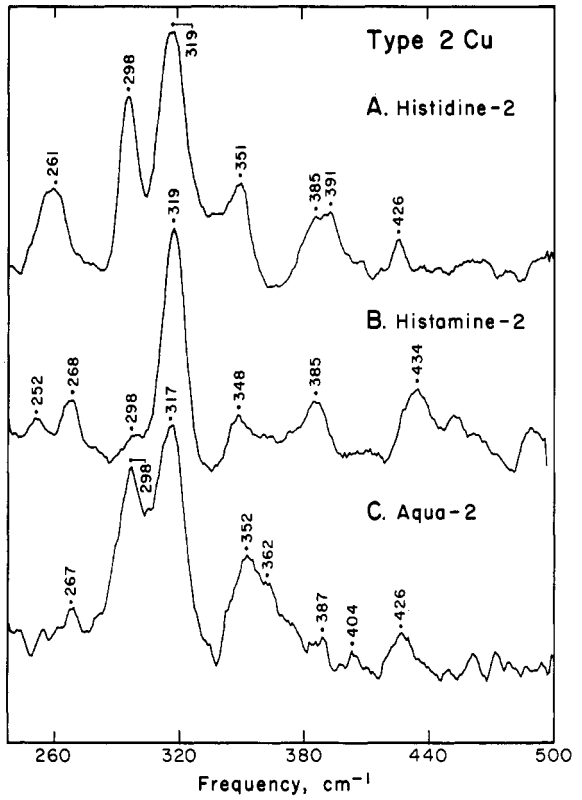


FIGURE 6: Resonance Raman spectra of type 2 sites in H117G azurins obtained with 413.1-nm excitation. (A) H117G plus histidine, (B) H117G plus histamine, and (C) H117G in $H_2O$ (no ligand added). Spectra were obtained on ~2 mM samples in MES buffer (pH 6.0) at 15 K using a power of 40 mW, resolution of 7 $cm^{-1}$, scan rate of 0.5 $cm^{-1}/s$, and accumulations of 5–13 scans.

Loehr, and G. W. Canters, unpublished results). Thus, the RR spectra of these type 2 species can be assigned to vibrations of the cysteinate ligand whose coplanar conformation continues to provide vibronic and kinematic coupling within the Cu–cysteinate moiety.

The major way in which the histidine-2 and histamine-2 species differ from their type 1 counterparts is that the maximum Raman intensity is associated with vibrational modes that are ~100 $cm^{-1}$ lower in energy (*vide infra*). In addition, the relative scattering intensity of the histidine-2 component with 413-nm excitation is <10% of that of the type 1 site in WT azurin with 647-nm excitation. Such weak RR scattering appears to be typical of Cu–thiolate complexes in the type 2 category (Han et al., 1993).

*Structure of Type 2 Complexes.* The tetragonal geometry of the histidine-2 and histamine-2 complexes of H117G azurin is evident from the blue shift of the major absorption bands to 400 nm as well as from the large EPR $A_\parallel$ values of ~160 × $10^{-4}$ $cm^{-1}$ (Table I). A number of well-characterized tetragonal or square-planar copper–thiolate complexes exhibit similarly intense thiolate → Cu(II) CT bands ($\epsilon$ >1000 $M^{-1}$ $cm^{-1}$) near 400 nm (High et al., 1979; Yamabe et al., 1982; Bharadwaj et al., 1986) and similarly large $A_\parallel$ values >140 × $10^{-4}$ $cm^{-1}$ (Addison, 1985). Such tetragonal coordination is generally accompanied by a lengthening of the Cu–S bond to 2.25–2.40 Å (Kitajima, 1993), compared to the typical value of 2.15 Å for a trigonal type 1 site (Han et al., 1991). This increased bond length is a consequence of changing the number of strongly coordinated ligands from three to four.

The occurrence of intense RR bands at lower energy in the histidine-2 and histamine-2 complexes of H117G azurin (Table II) is also suggestive of significant increases in their Cu–S bond lengths. In WT azurin, the RR modes at 372 and 408 $cm^{-1}$ undergo shifts of ~–1 $cm^{-1}$ upon substitution of $^{65}Cu$ for $^{63}Cu$ (Blair et al., 1985). Similar frequency shifts are observed for type 1 H117G reconstituted with Cu isotopes (Sanders-Loehr, 1993). However, reconstitution of H117G with Cu isotopes and histidine leads to a different isotope dependence (C. R. Andrew, J. Sanders-Loehr, and G. W. Canters, unpublished results). The histidine-2 component exhibits no Cu-isotope shifts for the peaks at 351, 385, 391, or 426 $cm^{-1}$, whereas its dominant peaks at 261, 298, and 319 $cm^{-1}$ do undergo shifts of –2.5, –0.8, and –0.5 $cm^{-1}$, respectively, with $^{65}Cu$ in place of $^{63}Cu$. Thus, the Cu–S stretch is coupling to cysteine ligand fundamentals near 300 $cm^{-1}$, a shift of ~100 $cm^{-1}$ to lower energy compared to WT. This explains why these bands have become the most intense features in the type 2 RR spectra (Figure 6).

According to Badger's rule (Herschbach & Laurie, 1961), a –100-$cm^{-1}$ shift in a pure Cu–S stretching frequency at 400 $cm^{-1}$ would correspond to an increase of ~0.2 Å in bond length (i.e., from 2.15 to 2.35 Å). This is certainly within the range of Cu–S bond lengths observed for type 2 Cu complexes (Han et al., 1993). Further evidence for a lengthening of the Cu–S(Cys) bond comes from the fact that the C–S stretch at 763 $cm^{-1}$ in the histidine-2 complex has shifted 10 $cm^{-1}$ to higher energy compared to the C–S stretch in WT azurin (Dave et al., 1993). Nevertheless, the shift in Raman frequencies provides only a rough approximation of the actual change in bond length because the Cu-isotope shifts are distributed over several modes and because changes in the Cu–S–C angle of the cysteinate ligand could also affect the vibrational coupling.

It is of interest to consider how the trigonal type 1 Cu site of H117G(Imid) has rearranged to a tetragonal type 2 Cu site in the presence of exogenous bidentate ligands. As with the previous examples, the azurin mutant with Asp in place of the Cys 112 ligand also appears to have produced a tetragonal type 2 site by virtue of the aspartate behaving as a bidentate ligand (Mizoguchi et al., 1992). Thus, the $(His)_2Cys$ ligand plane appears to be capable of accommodating a four-ligand set following removal of one of the three original ligands. A tetragonal structure which accounts for the properties of the histidine-2 and histamine-2 complexes is one in which a fourth strong ligand is added to the His–Cys–Imid ligand plane (Figure 1C). Having a fourth ligand inserted into the equatorial plane could help to explain the significant lengthening of the Cu–S bond. In contrast, other type 2 Cu sites such as those in the H46C and H120C mutants of superoxide dismutase have their maximum RR intensity closer to 350 $cm^{-1}$ (Han et al., 1993), indicating less perturbation of the copper thiolate.

*Type 1 and Type 2 with Aqua Ligands (pH 6.0).* Reconstitution of H117G azurin with Cu at pH 6.0 and no additional exogenous ligands also leads to a mixture of species. The electronic spectrum of His117Gly($H_2O$) shows a primary absorption band at 420 nm and a second component at 628 nm (Figure 2D, Table I). These spectra are reminiscent of H117G(His) and H117G(Hista), albeit with different energies and extinction coefficients. Resonance Raman spectroscopy verifies that the two absorption maxima are associated with two different species, aqua-1 and aqua-2.

Excitation of H117G($H_2O$) at 647.1 nm gives the RR spectrum of the aqua-1 component. Compared to WT, the mode at 372 $cm^{-1}$ has shifted 4 $cm^{-1}$ to lower energy, and the most intense features are now at 368 and 397 $cm^{-1}$. The similarity of the aqua-1 RR spectrum to those of the H117G

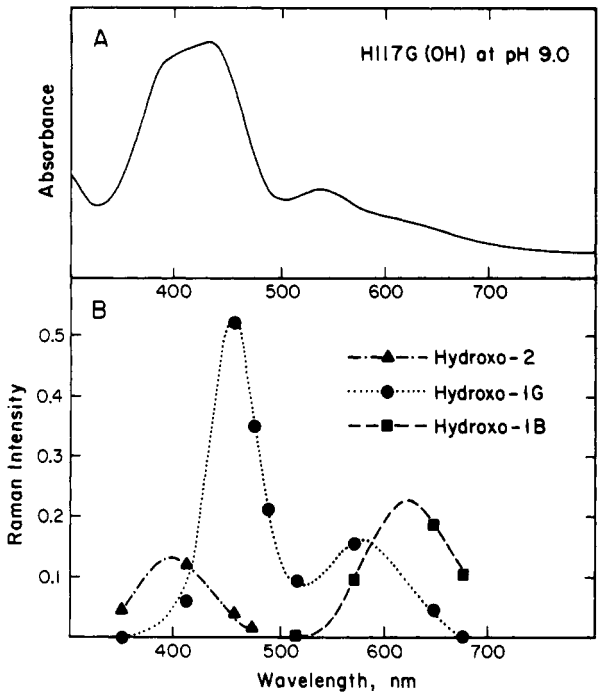


FIGURE 7: Absorption spectrum and resonance Raman excitation profiles for H117G(OH). (A) The absorption spectrum was obtained on 0.1 mM H117G(OH) at pH 9.0 and 293 K. (B) The RR spectra were obtained as in Figure 8. Raman peak heights at each excitation wavelength were quantitated relative to the height of the 230-$cm^{-1}$ ice mode. Peaks chosen as representative of the different species were (▲) 350 $cm^{-1}$ for the hydroxo-2 complex, (●) 365 $cm^{-1}$ for the hydroxo-1G complex (corrected for the spectral contribution from hydroxo-1B), and (■) 428 $cm^{-1}$ for the hydroxo-1B complex.

halide complexes (Figure 4D) suggests that a water molecule is coordinated in the equatorial ligand plane in place of His117, generating a tetrahedral type 1 Cu site. The RR spectrum of the aqua-1 component is unaffected by incubation of the protein in $H_2{}^{18}O$. This behavior is reminiscent of the lack of an isotope effect for H117G reconstituted with [$^{15}$N]imidazole (Sanders-Loehr, 1993) and again points to the type 1 RR spectra being dominated by Cu–cysteinate modes with little or no coupling of vibrational modes from the other Cu ligands.

Excitation of H117G($H_2O$) at 413.1 nm reveals the weakly enhanced RR spectrum of the aqua-2 component having its most intense peak at 317 $cm^{-1}$ (Figure 6C). This RR spectrum is reminiscent of the bidentate histidine-2 and histamine-2 complexes (Table II). The EPR spectrum of H117G($H_2O$) shows only a tetragonal type 2 component (Figure 3D, Table I). With the absorption intensity at 628 nm being 24% of that of WT, one would have expected some indication of the aqua-1 species in the EPR spectrum. However, optical spectra indicate that lowering the temperature tends to shift the equilibrium in favor of the aqua-2 species. This would help to explain the discrepancy since the reported electronic spectrum (Figure 2, Table I) was obtained at 298 K, whereas the EPR spectrum (Figure 3D) was obtained at 77 K. The appearance of intense features at 294 and 317 $cm^{-1}$ as well as $\nu$(C–S) at 768 $cm^{-1}$ is indicative of a lengthening of the Cu–S(Cys) bond in the aqua-2 species. Together with the EPR spectrum, these data suggest that the aqua-2 component contains a tetragonal type 2 Cu site. Since the equatorial plane in azurin appears to be capable of accommodating two exogenous ligands in the bidentate ligand complexes, it is plausible that two water molecules are similarly coordinated in the aqua-2 complex.

*Type 1 and Type 2 with Hydroxo Ligands (pH 9.0).* The electronic and RR spectra of WT azurin are independent of

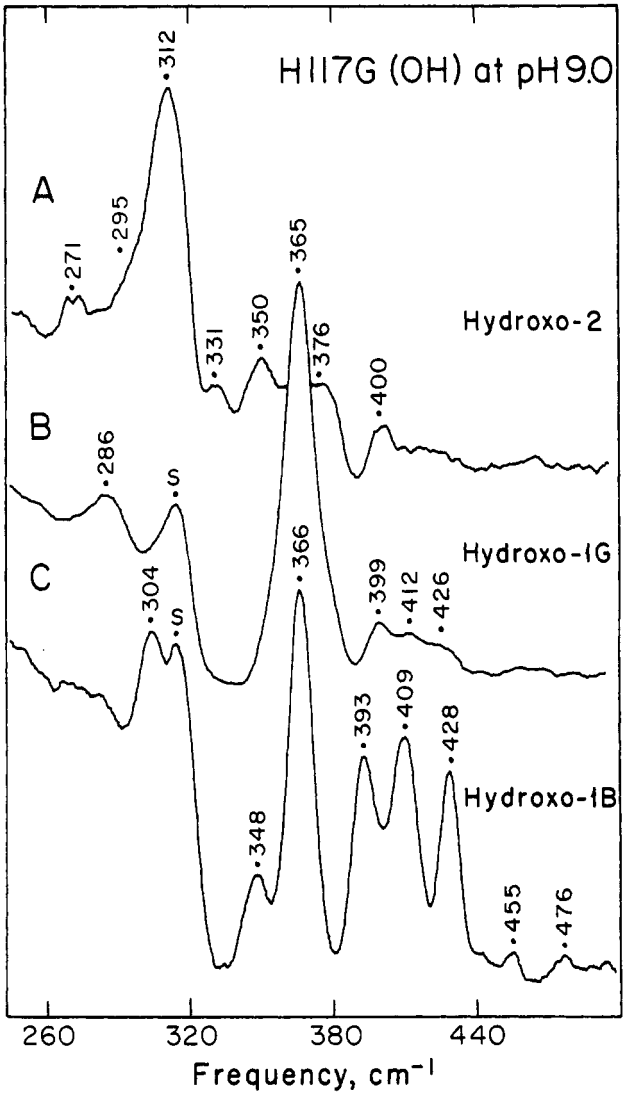


FIGURE 8: Resonance Raman spectra of H117G(OH) obtained at different excitation wavelengths. The protein sample (3 mM) in 20 mM CHES (pH 9.0) at 15 K was probed with excitation at (A) 413.1 nm (38 mW), (B) 457.9 nm (50 mW), and (C) 647.1 nm (100 mW) using 8-$cm^{-1}$ resolution and an accumulation of 25, 9, and 16 scans, respectively. Spectrum C contains a 25% contribution from the species in spectrum B.

pH in the range from 6 to 10 (van de Kamp et al., 1993). In contrast, H117G reconstituted with Cu (but without additional exogenous ligands) shows considerable spectroscopic variability with pH. As the pH is raised from 6.0 to 9.0, the band at 420 nm due to the aqua-2 component (Figure 2D) decreases in intensity and is replaced by three new absorption maxima at 400, 440, and 540 nm (Figure 7A). Within this same pH range, the intensity of the band at 628 nm due to the aqua-1 component also decreases in intensity ($pK_a$ = 8.2), and the absorption maximum shifts from 628 to 620 nm. Excitation within the different absorption bands produces a set of three distinct RR spectra (Figure 8) belonging to species designated as hydroxo-2, hydroxo-1G, and hydroxo-1B. The absorption bands associated with each of the three hydroxo complexes have been distinguished by plotting excitation profiles for representative peaks from each RR spectrum (Figure 7B).

The hydroxo-2 complex is probed by excitation at 413 nm, which produces a RR spectrum (Figure 8A) similar to those of the type 2 Cu complexes (Table II). The appearance of an intense peak at 312 $cm^{-1}$ with a shoulder at 295 $cm^{-1}$ is reminiscent of the RR spectrum of the histamine-2 complex (Figure 6B) and indicative of a lengthening of the Cu–S(Cys)

bond. The excitation profile for the hydroxo-2 complex (monitored by the 350-$cm^{-1}$ peak that is unique to this species) shows that its Raman spectrum is in resonance with the 400-nm absorption band (Figure 7B). This absorption maximum is also typical of a type 2 Cu species (Table I). Thus, the hydroxo-2 component is likely to have a tetragonal type 2 site (Figure 1C) with two hydroxo ligands (or aqua plus hydroxo) in the equatorial ligand plane.

The hydroxo-1B complex is probed by excitation of H117G-(OH) at 647 nm (Figure 8C) and reveals a RR spectrum characteristic of an anionic type 1 Cu complex (Table II). The occurrence of five prominent peaks between 348 and 428 $cm^{-1}$ with the greatest intensity at 366 $cm^{-1}$ is particularly close to the RR spectrum of the $N_3^-$ complex of H117G (Figure 4F). (The intensity of the 366-$cm^{-1}$ peak in Figure 8C is, however, exaggerated due to a 25% contribution from the hydroxo-1G complex.) The excitation profile for the hydroxo-1B complex (followed by the well-isolated peak at 428 $cm^{-1}$) reveals that this Raman spectrum is enhanced only by excitation within the 620-nm absorption band. Thus, the hydroxo-1B complex can be characterized as having a *blue type 1 Cu site* and is most likely to have a trigonal geometry (Figure 1A) with a hydroxo ligand in the equatorial ligand plane.

Finally, excitation of H117G(OH) at either 458 nm (Figure 8B) or 570 nm (data not shown) produces a RR spectrum which is dominated by a peak at 365 $cm^{-1}$, with a set of weaker features at 399, 412, and 426 $cm^{-1}$ that differ in frequency from the peaks in Figure 8A,C. This RR spectrum is still characteristic of a type 1 Cu site and is assigned to a hydroxo-1G component. The excitation profile for the 365-$cm^{-1}$ peak (corrected for the contribution from the hydroxo-1B component) shows that this spectrum is in resonance with both the 440- and 540-nm absorption bands. Because these two absorption bands originate from a single species which is the major component of H117G(OH), the hydroxo-1G complex can be described as having a *green type 1 Cu site*.

The hydroxo-1G complex with an intense absorption at 440 nm and a smaller band at 540 nm is reminiscent of other green type 1 Cu proteins: nitrite reductase (NiR) and a mutant superoxide dismutase (SOD). NiR from *Achromobacter cycloclastes* (Libby & Averill, 1992) has its major absorption at 458 nm ($\epsilon$ = 2530 $M^{-1}$ $cm^{-1}$), a weaker component at 585 nm ($\epsilon$ = 1890 $M^{-1}$ $cm^{-1}$), and a tetrahedral type 1 Cu site [as revealed by the crystal structure of Godden et al. (1991)]. For the zinc-site H80C mutant of SOD, binding of Cu in the Zn site produces intense absorption bands at 459 and 595 nm (both with $\epsilon > 1400$ $M^{-1}$ $cm^{-1}$) (Lu et al., 1992). Analysis of a series of type 1 Cu proteins reveals that increased absorbance near 460 nm is correlated with increased rhombicity in the EPR spectrum and that both properties are likely to be due to increased tetrahedral character in the type 1 site (Han et al., 1993; Lu et al., 1993). The RR spectra of NiR and mutant SOD are each dominated by a strong mode at 361 and 352 $cm^{-1}$, respectively, with the modes to higher energy being considerably weaker than in other type 1 Cu sites (Han et al., 1993). This same pattern is observed in the RR spectrum of the hydroxo-1G complex of H117G azurin (Figure 7B), strongly suggesting that it, too, contains a tetrahedral type 1 Cu site.

## CONCLUSIONS

Studies of His117Gly azurin have demonstrated that removal of a histidine ligand from a type 1 Cu site leads to a surprising flexibility in the coordination geometry. The various species are readily characterized by RR spectroscopy, where *shifts in vibrational intensities are indicative of changes in Cu–S(Cys) bond length*. Thus, when the geometry changes from a trigonal type 1 to tetrahedral type 1 site, the Cu–S(Cys) stretch shows greater coupling with vibrational fundamentals that are 10–40-$cm^{-1}$ lower in energy. The geometry change to a tetragonal type 2 site is accompanied by an even greater lengthening of the Cu–S(Cys) bond due to the coordination of a fourth ligand in the equatorial plane, and the Cu–S(Cys) stretch now couples with vibrational modes that are ~100 $cm^{-1}$ lower in energy relative to those of a trigonal type 1 site.

(1) Addition of exogenous imidazole to H117G azurin regenerates a trigonal type 1 Cu site whose RR spectrum is essentially identical to that of WT.

(2) Addition of exogenous anions such as $Cl^-$, $Br^-$, $SCN^-$, and $N_3^-$ in place of imidazole still generates a type 1 Cu site. The RR spectra show this to be accompanied by a lengthening of the Cu–S(Cys) bond, most likely due to a distortion toward tetrahedral geometry. The fact that the vibrational frequencies in the 350–500-$cm^{-1}$ region are so little affected by the replacement of either histidine ligand (117 or 46) demonstrates that the RR spectrum is due primarily to the Cu–cysteinate moiety.

(3) Addition of bidentate ligands such as histidine and histamine leads to a mixture of type 1 and type 2 species. The type 1 components ($\lambda_{max}$ at 634 nm), with only the imidazole moiety ligated, have RR spectra typical of a trigonal type 1 site with the most intense feature at 410 $cm^{-1}$. The type 2 components ($\lambda_{max}$ at 400 nm), with both the imidazole and amine nitrogen atoms coordinated, exhibit RR spectra in which the most intense spectral features have shifted to the 300-$cm^{-1}$ region, as expected for an increase of ~0.2 Å in Cu–S(Cys) bond length.

(4) In the absence of exogenous ligands, the H117G mutant forms another type 2 species at pH 6 that is most likely due to the presence of two coordinated water molecules in the equatorial ligand plane. At pH 9, three different species are observed, all likely to contain hydroxo ligands. There is a type 2 species whose RR and electronic spectra ($\lambda_{max}$ at 400 nm) are similar to that of H117G with bidentate histidine; a trigonal type 1 species whose RR and electronic spectra ($\lambda_{max}$ at 620 nm) is similar to that of H117G with azide; and a tetrahedral type 1 species whose RR and electronic spectra ($\lambda_{max}$ at 440 nm) are similar to those of nitrite reductase.

(5) The ability of the H117G mutant to accommodate such a variety of coordination geometries implies that the protein can adopt several different stable Cu-site conformations. In contrast, WT azurin appears to have only one stable Cu-site conformation which helps to promote rapid interconversion between Cu(I) and Cu(II).

## ACKNOWLEDGMENT

We are grateful to Drs. Roman Czernuszewicz, Colin Andrew, and Herbert Nar for making data available prior to publication and for many helpful discussions.

## REFERENCES

Addison, A. W. (1985) in *Copper Coordination Chemistry: Biochemical and Inorganic Perspectives* (Karlin, K. D., & Zubieta, J., Eds.) pp 109–128, Adenine Press, New York.

Adman, E. T. (1985) in *Topics in Molecular and Structural Biology. Part 1. Metalloproteins* (Harrison, P. M., Ed.) pp 1–42, VCH Verlagsgesellschaft, Weinheim.

Adman, E. T. (1991) *Adv. Protein Chem. 42*, 145–197.

Baker, E. N. (1988) *J. Mol. Biol. 203*, 1071–1095.
Bharadwaj, P, K., Potenza, J. A., & Schugar, H. J. (1986) *J. Am. Chem. Soc. 108*, 1351–1352.
Blair, D. F., Campbell, G. W., Schoonover, J. R., Chan, S. I., Gray, H. B., Malmström, B. G., Pecht, I., Swanson, B. I., Woodruff, W. H., Cho, W. K., English, A. M., Fry, H. A., Lum, V., & Norton, K. A. (1985) *J. Am. Chem. Soc. 107*, 5755–5766.
Chang, T. K., Iverson, S. A., Rodrigues, C. G., Lew, A. Y. C., Germanas, J. P., & Richards, J. H. (1991) *Proc. Natl. Acad. Sci. U.S.A. 88*, 1325–1329.
Church, W. B., Guss, J. M., Potter, J. J., & Freeman, H. C. (1986) *J. Biol. Chem. 261*, 234-237.
Dave, B. C., Germanas, J. P., & Czernuszewicz, R. S. (1993) *J. Am. Chem. Soc.* (in press).
den Blaauwen, T., & Canters, G. W. (1993) *J. Am. Chem. Soc. 115*, 1121–1129.
den Blaauwen, T., van de Kamp, M., & Canters, G. W. (1991) *J. Am. Chem. Soc. 113*, 5050-5052.
Garrett, T. P. J., Clingeleffer, D. J., Guss, J. M., Rogers, S. J., & Freeman, H. C. (1984) *J. Biol. Chem. 259*, 2822–2825.
Germanas, J. P., Di Bilio, A. J., Gray, H. B., & Richards, J. H. (1993) *Biochemistry 32*, 7698–7702.
Godden, J. W., Turley, S., Teller, D. C., Adman, E. T., Liu, M. Y., Payne, W. J., & LeGall, J. (1991) *Science 253*, 438–442.
Gray, H. B., & Malmström, B. G. (1983) *Comments Inorg. Chem. 2*, 203–209.
Guss, J. M., Bartunik, H. D., & Freeman, H. C. (1992) *Acta Crystallogr. B48*, 790–811.
Han, J., Adman, E. T., Beppu, T., Codd, R., Freeman, H. C., Huq, L., Loehr, T. M., & Sanders-Loehr, J. (1991) *Biochemistry 30*, 10904–10913.
Han, J., Loehr, T. M., Lu, Y., Valentine, J. S., Averill, B. A., & Sanders-Loehr, J. (1993) *J. Am. Chem. Soc. 115*, 4256–4263.
Herschbach, D. R., & Laurie, V. W. (1961) *J. Chem. Phys. 35*, 458–463.
Hoitink, C. W. G., & Canters, G. W. (1992) *J. Biol. Chem. 267*, 13836–13842.
Hughey, J. L., IV, Fawcett, T. G., Rudich, S. M., Lalancette, R. A., Potenza, J. A., & Schugar, H. J. (1979) *J. Am. Chem. Soc. 101*, 2617–2623.
Karlsson, B. G., Nordlin, M., Pascher, T., Tsai, L-C., Sjölin, L., & Lundberg, L. G. (1991) *Protein Eng. 4*, 343–349.
Kitajima, N. (1993) *Adv. Inorg. Chem. 39*, 1–77.
Libby, E., & Averill, B. A. (1992) *Biochem. Biophys. Res. Commun. 187*, 1529–1535.
Lowery, M. D., & Solomon, E. I. (1992) *Inorg. Chim. Acta 198–200*, 233–243.
Lu, Y., Gralla, E. B., Roe, J. A., & Valentine, J. S. (1992) *J. Am. Chem. Soc. 114*, 3560–3562.
Lu, Y., LaCroix, L. B., Lowery, M. D., Solomon, E. I., Bender, C. J., Peisach, J., Roe, J. A., Gralla, E. B., & Valentine, J. S. (1993) *J. Am. Chem. Soc. 115*, 5907–5918.
Mizoguchi, T. J., Di Bilio, A. J., Gray, H. B., & Richards, J. H. (1992) *J. Am. Chem. Soc. 114*, 10076–10078.
Nar, H., Messerschmidt, A., Huber, R., van de Kamp, M., Canters, G. W. (1991a) *J. Mol. Biol. 218*, 427–447.
Nar, H., Messerschmidt, A., Huber, R., van de Kamp, M., & Canters, G. W. (1991b) *J. Mol. Biol. 221*, 765–772.
Nar, H., Huber, R., Messerschmidt, A., Filipou, A. C., Barth, M., Jaquinod, M., van de Kamp, M., & Canters, G. W. (1992) *Eur. J. Biochem. 205*, 1123–1129.
Nestor, L., Larrabee, J. A., Woolery, G., Reinhammar, B., & Spiro, T. G. (1984) *Biochemistry 23*, 1084–1093.
Nishimura, Y., Hirakawa, A. Y., & Tsuboi, M. (1978) *Adv. Infrared Raman Spectrosc. 5*, 217-275.
Pate, J. E., Ross, P. K., Thamann, T. J., Reed, C. A., Karlin, K. D., Sorrell, T. N., & Solomon, E. I. (1989) *J. Am. Chem. Soc. 111*, 5198–5209.
Romero, A., Hoitink, C. W. G., Nar, H., Huber, R., Messerschmidt, A., & Canters, G. W. (1993) *J. Mol. Biol. 229*, 1007–1021.
Sanders-Loehr, J. (1993) in *Bioinorganic Chemistry of Copper* (Karlin, K. D., & Tyeklar, Z., Eds.) pp 51–63, Chapman & Hall, New York.
Shepard, W. E. B., Anderson, B. F., Lewandoski, D. A., Norris, G. E., & Baker, E. N. (1990) *J. Am. Chem. Soc. 112*, 7817–7819.
Solomon, E. I., Baldwin, M. J., & Lowery, M. D. (1992) *Chem. Rev. 92*, 521–542.
Sykes, A. G. (1991) *Adv. Inorg. Chem. 36*, 377–408.
Thamann, T. J., Frank, P., Willis, L. J., & Loehr, T. M. (1982) *Proc. Natl. Acad. Sci. U.S.A. 79*, 6396–6400.
van de Kamp, M., Silvestrini, M. C., Brunori, M., Van Beeumen, J., Hali, F. C., & Canters, G. W. (1990a) *Eur. J. Biochem. 194*, 109–118.
van de Kamp, M., Floris, R., Hali, F. C., & Canters, G. W. (1990b) *J. Chem. Soc. 112*, 907–908.
van de Kamp, M., Canters, G. W., Andrew, C. R., & Sanders-Loehr, J. (1993) *Eur. J. Biochem.* (in press).
Williams, R. J. P. (1971) *Inorg. Chim. Acta Rev. 5*, 137.
Yamabe, T., Hori, K., Minato, T., Fukui, K., & Sugiura, Y. (1982) *Inorg. Chem. 21*, 2040–2046.